# Nanomolar Inhibitors of the Peptidyl Prolyl Cis/Trans Isomerase Pin1 from Combinatorial Peptide Libraries

Dirk Wildemann,[†] Frank Erdmann,[†] Birte Hernandez Alvarez,[†,‡] Gerlind Stoller,[†] Xiao Z. Zhou,[§] Jörg Fanghänel,[†] Mike Schutkowski,[†,||] Kun P. Lu,[§] and Gunter Fischer[†,*]

*Max Planck Research Unit for Enzymology of Protein Folding, Weinbergweg 22, 06120 Halle/Saale, Germany, Max Planck Institute for Developmental Biology, Department Protein Evolution, Spemannstrasse 35, 72076 Tuebingen, Germany, Cancer Biology Program, Department of Medicine, Beth Israel Deaconess Medical Center, Harvard Medical School, Boston, Massachusetts 02115, and Jerini AG, Invalidenstrasse 130, 10115 Berlin, Germany*

*Received January 12, 2006*

**Abstract:** The peptidyl prolyl cis/trans isomerase Pin1 has been implicated in the development of cancer, Alzheimer's disease and asthma, but highly specific and potent Pin1 inhibitors remain to be identified. Here, by screening a combinatorial peptide library, we identified a series of nanomolar peptidic inhibitors. Nonproteinogenic amino acids, incorporated into 5-mer to 8-mer oligopeptides containing a D-phosphothreonine as a central template, yielded selective inhibitors that blocked cell cycle progression in HeLa cells in a dose-dependent manner.

Protein phosphorylation on Ser/Thr-Pro moieties by proline-directed protein kinases and dephosphorylation of *O*-phosphoserine (Ser($PO_3H_2$))-Pro and *O*-phosphothreonine (Thr($PO_3H_2$))-Pro motifs by protein phosphatases play a prominent role in controlling transcription, cell differentiation, and proliferation.[1,2] In addition to its phosphorylation state, the peptidyl prolyl bond of the Ser/Thr-Pro moiety itself behaves as a molecular switch in that two energetically favorable conformational states, the cis and the trans prolyl isomers, are separated by a high rotational energy barrier. Such a barrier in conformational interconversion of Ser($PO_3H_2$)/Thr($PO_3H_2$)-Pro segments in substrate proteins can be overcome by the peptidyl prolyl cis/trans isomerase (PPIase) Pinl. Pin1 substrate proteins often have distinct native states with different biological activity, energetically separated by the prolyl bond isomerism.[1,3−5] Pin1-catalyzed isomerization is now known to comprise a novel regulatory mechanism for the post-phosphorylative activity of signal transduction proteins.[2] In this respect Pin1 is involved in cell cycle regulation, transcription, and response to DNA damage, and it is a key mediator in the asthma-relevant production of GM-CSF.[2,6−9] The enzyme also plays a role in the development of Alzheimer's disease[2] and different types of solid cancer, e.g. colon, prostate, lung, breast, and squamous cell carcinomas as well as sarcomas such as lymphomas and melanomas. In the cancer-related cases, Pin1 overexpression leads to the upregulation of several oncogens by multiple pathways.[2,10,11] Pin1-targeted RNAi experiments in prostate cancer cells suggested a role for Pin1 in both tumor genesis and maintenance of the transformed phenotype.[12] Several reports have indicated Pin1 to be a potential anticancer drug target. Depletion of Pin1 in various human cancer cell lines induces mitotic arrest and initiates apoptosis.[2,6,13] Importantly, inhibition of Pin1 may have less toxic effects on noncancerous cells, as Pin1 knockout mice are viable and show only minimal abnormalities after long lifetimes.[7] However, extremely low cellular levels of ESS1, the yeast Pin1 homologue, were found to be required and sufficient for optimal growth of yeast.[14] Only 1.5−20 ESS1 molecules per cell sufficed for growth. Thus, only a low nanomolar inhibition constant preconditions a small-molecule Pin1 inhibitor to substantiate a depletion of activity in excess of 99%, at tolerable doses for in vivo applications. Pin1 belongs to the parvulin family of PPIases and consists of two phosphopeptide-binding domains, a type IV WW domain and a parvulin-like catalytic domain.[6] To date, several reversible inhibitors of the Pin1 PPIase activity have been reported that show $K_i$ values in the micromolar range.[15−17] Uchida et al. showed that cancer cell lines expressing a particularly high level of Pin1 are more sensitive toward such inhibitors compared to other cancer cell lines.[17] These inhibitors showed an antiproliferative activity on cancer cells in line with the studies on Pin1 depletion mentioned above. However, as irreversible Pin1 inhibitors, juglone and pepticinnamines proved to be unspecific. Juglone was found to block RNA polymerase II-mediated transcription presumably independent of Pin1 inhibition.[18−20]

Here, we describe reversible *h*Pin1 inhibitors with affinities in the nanomolar range. The compounds, developed by screening a cellulose-bound combinatorial peptide library for binding of recombinant *h*Pin1, show a clear preference for interaction with the PPIase domain over the second phosphopeptide-specific binding domain. The library was prepared by standard automated spot synthesis and was composed of 5-mer N-acetylated peptides conforming to the general structure Ac-Xaa-Thr($PO_3H_2$)-Yaa-Zaa-NHCH($(CH_2)_2$CONH-linker)COOH. This basic structure was derived from the known substrate recognition preferences of the *h*Pin1 catalytic site.[4] The invariant side chain N-alkylated glutamine residue originates from side chain condensation of glutamic acid via the free amino group of the cellulose matrix-bound $\beta$-alanyl-$\beta$-alanine linker. In addition to phenylalanine, nine unnatural hydrophobic amino acids for Zaa and Xaa (Abz, Bip, Bth, Cha, Dbg, Nal, tBuGly, tBuPhe, Thi)[a] and eight *N*-alkyl amino acids for Yaa (MeAla, MePhe, Pia, Pip, 4Pip, Thz, Tic, Pro) were utilized in order to manipulate proteolytic stability and *h*Pin1 affinity simultaneously. The presence of proline surrogates, *N*-alkyl, and other unnatural amino acids in FK506, rapamycin, and cyclosporine A was shown to have a major impact on their inhibitory effects on members of other PPIases families. Generally, natural amino acids in the position following proline render oligopeptides less suitable for tight interaction with the active site of Pin1.[15] Furthermore, we included 4-aminomethylcyclohexanecarboxylic acid and 4-aminomethylbenzoic acid for substitution in position Yaa to investigate whether secondary amide bonds formed by an

* To whom correspondence should be addressed. E-mail: fischer@enzyme-halle.mpg.de. Phone: +49-345-5522800. Fax: +49−345−5511972.

[†] Max Planck Research Unit for Enzymology of Protein Folding.

[‡] Max Planck Institute for Developmental Biology.

[§] Harvard Medical School.

[||] Jerini AG.

[a] Abbreviations: Abz, 2-aminobenzoic acid; Bip, $\beta$-(4-biphenylyl)alanine; Bth, $\beta$-(3-benzothienyl)alanine; Cha, $\beta$-cyclohexylalanine; Dbg, $\alpha,\alpha$-dibutylglycine; MeAla, $N^{\alpha}$-methylalanine; MePhe, $N^{\alpha}$-methylphenylalanine; Nal, $\beta$-(2-naphthyl)alanine; Pia, 4-piperidinylacetic acid; Pip, piperidine-2-carboxylic acid; 4Pip, piperidine-4-carboxylic acid; tBuGly, $\alpha$-*tert*-butylglycine; tBuPhe, $\alpha$-*tert*-butylphenylalanine; Thi, $\beta$-(2-thienyl)alanine; Thz, thiazolidine-4-carboxylic acid; Tic, 1,2,3,4-tetrahydro-isoquinoline-3-carboxylic acid.

10.1021/jm060036n CCC: $33.50 
Published on Web 03/17/2006

**Table 1.** Inhibition of the *h*Pin1 PPIase Activity by Peptides with the General Sequence
Ac-Lys($N^{\epsilon}$-biotinoyl)-Ala-Ala-Xaa-Thr($PO_3H_2$)-Yaa-Zaa-Gln-$NH_2$

| | residues in position | | | |
|---|---|---|---|---|
| Pin1 ligand | Xaa | Yaa | Zaa | Pin1 inhibition: $IC_{50}$ ($\mu$M)[a] |
| **1** | tBuPhe | Pro | Nal | 30 ± 1.8 |
| **2** | Thi | Pro | Bip | 22 ± 1.5 |
| **3** | Bth | Pro | Cha | >50 |
| **4** | Bth | Pro | Nal | 20 ± 1.6 |
| **5** | Bip | Pro | Bth | 15 ± 0.8 |
| **6** | Bip | Pro | Nal | 18 ± 1.1 |
| **7** | Nal | Pro | tBuGly | >50 |
| **8** | Nal | Pro | Cha | >50 |
| **9** | tBuPhe | MeAla | Nal | 10 ± 0.4 |
| **10** | Thi | MeAla | Nal | 15 ± 0.8 |
| **11** | Cha | MeAla | Nal | 7 ± 0.4 |
| **12** | Phe | MeAla | Bth | 20 ± 1.7 |
| **13** | tBuPhe | Tic | Bth | 8 ± 0.4 |
| **14** | Cha | Tic | Nal | 25 ± 1.5 |
| **15** | Bth | Pip | Nal | 0.21 ± 0.01 |

[a] $IC_{50}$ values were determined using the protease free PPIase assay.[15] Abz-Ala-Glu-Pro-Phe-NH-Np was used as substrate. Measurements were done in 35 mM HEPES buffer (pH 7.8) at 10 °C.Kinetic measurements and the synthesis of the peptides are described in detail in the Supporting Information.

aminomethyl group attached to a six-membered ring could fit into the proline binding pocket of *h*Pin1.

For first-round screening experiments, the recombinant *h*Pin1 catalytic domain was used in isolation in order to avoid potential specificity problems associated with the known phosphopeptide affinity of the WW domain.[21] The loaded cellulose membranes were screened by application of soluble *h*Pin1 catalytic domain, which was then detected on the spots by Western blotting (see Supporting Information). The read-out of the oligopeptide library thus displays Pin1 binding to the peptide spots. Library screening revealed exceptional sensitivity of position Zaa for *h*Pin1 PPIase domain binding, as α-*tert*-butylglycine, α,α-dibutylglycine, and 2-aminobenzoic acid are not at all tolerated. In contrast, *β*-(4-biphenylyl)alanine, *β*-(3-benzothienyl)alanine and *β*-(2-naphthyl)alanine at the Zaa position represent strongly preferred residues. The position Xaa accepted the whole spectrum of hydrophobic amino acid derivatives.

A PPIase activity assay of *h*Pin1 indicated that the Pin1 affinities obtained with the cellulose-bound peptides by visual inspection correlate well with the inhibitory power of corresponding soluble peptides. For the soluble peptides a Gln residue substitutes for the matrix-anchored glutamic acid. To validate the relationship between cellulose matrix-derived Pin1 binding and Pin1 inhibition for a broad range of separate screening spots, a number of strong and weak binders from our library were synthesized as soluble peptides.

Initially, a total of fifteen compounds of the general structure Ac-Lys($N^{\epsilon}$-biotinoyl)-Ala-Ala-Xaa-Thr($PO_3H_2$)-Yaa-Zaa-Gln-$NH_2$ (Table 1) were generated to serve as starting points for final design. The N-terminal extension converts the *h*Pin1 PPIase domain binding peptides of the cellulose-bound library to biotin-labeled molecules that allow pull-down experiments with streptavidin-coated beads. Obviously, this modification does not impede the inhibition of *h*Pin1 PPIase activity. The lowest $IC_{50}$ value of 210 ± 10 nM was found for **15**, which contains a piperidine-2-carboxylic acid at position Yaa. A prolyl residue at this position (peptide **4**) caused a 100 fold decrease of inhibition, indicating tightly regulated active site geometry of *h*Pin1 at the P1' position of the substrate-like inhibitor. Peptide **15** at 500 $\mu$M concentration does not show significant *h*Pin1 inhibition (residual PPIase activity ≥95%) when the phosphoester group on threonine is lacking (data not shown). Structure-affinity relationships revealed that Pip is exceptional in inducing a high affinity conformation of octapeptides for Pin1 (Table 1). The Pip effect is independent of peptide chain length (Table 2). Insight into the molecular basis of this effect must await information about the three-dimensional structure of a Pin1/Pip−peptide complex.

**Table 2.** Inhibition of the *h*Pin1 PPIase Activity by Peptides of Different Chain Length

| Pin1 ligand | sequence | $K_i$ (nM)[a] |
|---|---|---|
| **15** | Ac-Lys($N^{\epsilon}$-biotinoyl)-Ala-Ala-Bth-Thr($PO_3H_2$)-Pip-Nal-Gln-$NH_2$ | 183 ± 12 |
| **16** | Ac-Lys($N^{\epsilon}$-biotinoyl)-Ala-Ala-Bth-D-Thr($PO_3H_2$)-Pip-Nal-Gln-$NH_2$ | 1.2 ± 0.06 |
| **17** | Ac-Phe-D-Thr($PO_3H_2$)-Pip-Nal-Gln-$NH_2$ | 18.3 ± 1.3 |
| **18** | Ac-Phe-Thr($PO_3H_2$)-Pip-Nal-Gln-$NH_2$ | 547 ± 24 |
| **19** | Ac-Bth-Thr($PO_3H_2$)-Pip-Nal-Gln-$NH_2$ | 258 ± 13 |
| **20** | Ac-Lys($N^{\epsilon}$-biotinoyl)-Ala-Ala-Phe-D-Thr($PO_3H_2$)-Pip-Nal-Gln-$NH_2$ | 4.8 ± 0.4 |

[a] $K_i$ values were determined using the protease free PPIase assay.[15] Abz-Ala-Glu-Pro-Phe-NH-Np was used as substrate. Measurements were done in 35 mM HEPES buffer (pH 7.8) at 10 °C.Kinetic measurements and the synthesis of the peptides are described in detail in the Supporting Information.

Full-length *h*Pin1 exhibits two phosphopeptide-binding sites, one of which is not critical for enzyme activity. To distinguish whether **15** also interacts with the Pin1 WW domain, we performed far Western blot analyses using GST-coupled domain constructs of *h*Pin1. Accordingly, GST-*h*Pin1 (full length protein) and the single-domain constructs GST-*h*Pin1 PPIase domain and GST-*h*Pin1 WW domain were spotted separately onto nitrocellulose membranes and incubated with **15**. Specific binding of **15** was then detected using horseradish peroxidase-conjugated streptavidin. Figure 1A documents that **15** binds only to GST-*h*Pin1 and GST-*h*Pin1 PPIase domain but not to GST-WW domain. As expected, full length GST-*h*Pin1 and the GST-*h*Pin1 PPIase domain exhibit similar affinities, validated by visual inspection, whereas the peptide lacking the phosphate group was not able to form a complex with GST-*h*Pin1. To study how *h*Pin1 residues dictate affinity for **15**, point-mutated GST-*h*Pin1 variants were applied in far Western blotting experiments (Figure 1B). High binding capacity parallels residual PPIase activity of the *h*Pin1 variants, supporting the view that the active site blockade by **15** may, in fact, resemble those described by known competitive substrates. To examine its in vivo stability, **15** was incubated in HeLa cell lysates in absence of phosphatase and protease inhibitors. After 5 h of incubation, the respective mixture was extracted using streptavidin Sepharose. The extracted, biotin-conjugated compounds were analyzed by mass spectrometry. Only the dephosphorylated derivative of **15** was found, indicating that the sequence integrity of the peptide was maintained. Logically, when phosphatase inhibitors were added to the cell lysates, **15** was found to be stable over the incubation period.

Importantly, however, the D-Ser(Thr)($PO_3H_2$) moiety has been shown to be inert toward cellular phosphatases.[15] Similarly, the D-Thr($PO_3H_2$) residue at position P1, that is present in **16** (Table 2), was found to be advantageous for conversion of the inhibitor **15** into a cytosolically stable compound. A truncated version of **16**, reflected in **17**, served to optimize the diffusion process of the inhibitor in in vivo experiments. Detailed comparisons of inhibitors must take tight-binding of reactants into account. Therefore, $K_i$ values were measured instead of $IC_{50}$ values (Table 2). Importantly, a comparison of the $K_i$ values of **16** and **17** with their L-Thr($PO_3H_2$) congeners, summarized in Table 2, shows that reversion of the $C^{\alpha}$-stereocenter of the L-Thr($PO_3H_2$)

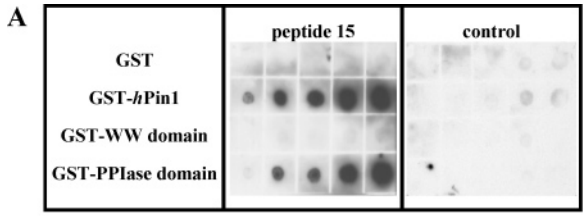


B

| peptide 15 (pmol) 1 5 10 52.5 105 | *h*Pin1 variant | PPIase activity (%) |
|---|---|---|
| | GST-*h*Pin1 | 100 [a] |
| | GST-*h*Pin1 K63A | 0.2 [a] |
| | GST-*h*Pin1 S67E | 0.3 [a] |
| | GST-*h*Pin1 R68, 69A | 0.4 [a] |
| | GST-*h*Pin1 C113A | 6.0 [a] |
| | GST-*h*Pin1 S16E | 100 [c] |
| | GST-*h*Pin1 H59A | 5.7 [b] |
| | GST-*h*Pin1 S154F | 35 [a] |

**Figure 1.** A. Binding preferences of the PPIase and WW domain of *h*Pin1 regarding **15.** Increasing amounts (from left to right: 1, 5, 10, 52.5, 105 pmol) of GST, GST-*h*Pin1, or its single GST-*h*Pin1 PPIase and GST-*h*Pin1 WW domain were spotted onto nitrocellulose membranes followed by a blocking procedure. The membranes were then incubated with a 1 $\mu$M solution of **15** or with a 50 $\mu$M solution of its nonphosphorylated derivative (control). Signals were detected after incubation of the nitrocellulose membranes with horseradish peroxidase-conjugated streptavidin followed by a chemiluminescent reaction using the SuperSignal substrate. B. Analysis of the binding of **15** to different GST-*h*Pin1 variants. Indicated amounts of **15** were spotted onto nitrocellulose membranes followed by a blocking procedure and incubation with the respective GST-*h*Pin1 variant (40 nM). To specifically detect the bound protein, the membranes were incubated with an anti *h*Pin1 PPIase domain antiserum as primary antibody and horseradish peroxidase-conjugated secondary antibody. Visualization was done using the SuperSignal substrate. Dilution series of the GST-conjugated *h*Pin1 variants, spotted onto nitrocellulose membranes, were used to verify similar affinities of binding of the primary antibody to the different Pin1 variants (data not shown). [a,b]Residual PPIase activities of GST-*h*Pin1 and its variants were according to Zhou *et al.* or Yaffe et al.[1,4] [c]The PPIase activity of the GST-*h*Pin1 variant S16E was measured in the protease free PPIase assay using Abz-Ala-Glu-Pro-Phe-NH−Np as substrate.[15] Experimental procedures are described in detail in the Supporting Information.

residue caused a marked reduction in $K_i$. With $K_i$ values of 1.2 and 18.3 nM, respectively, **16** and **17** represent the most potent Pin1 inhibitors available to date. As can be inferred from the data from **18**, **19**, and **20**, a biotin-conjugated linker and the substitution of the $\beta$-(3-benzothienyl)alanine by phenylalanine have only a minor influence on $K_i$. It should further be mentioned, that both **16** and **17**, and probably all other peptides described in Tables 1 and 2, inhibit Pin1 in a reversible manner. This was implied by the regain of the enzymatic activity observed after dialysis of mixtures containing the completely inhibited Pin1, an effect that results from dissociation of the *h*Pin1/**16** or *h*Pin1/**17** complex, respectively (data not shown).

Stability of **16** in cell lysates were examined as described above. High stability of **16** in the lysate was detected by

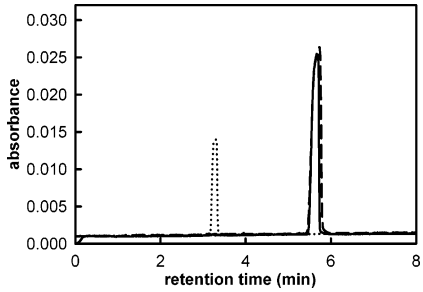


**Figure 2.** Stability of **17** in HeLa cell lysates was analyzed by capillary electrophoresis. Dashed line: Peptide **17** (5 $\mu$M) after 5 h of incubation in HeLa cell lysate (whole cell lysate of HeLa cells). Solid line: reference sample of **17** (5 $\mu$M) dissolved in pure separation buffer. The similar peak intensities of both samples indicate that **17** was not degradated in the cell lysate during the time of incubation. Dotted line: a reference sample containing the nonphosphorylated derivative of **17** (2 $\mu$M). 50 mM sodium phosphate buffer (pH 7.0) was used as separation buffer. Detection wavelength was 220 nm (experimental details are described in the Supporting Information).

extracting the intact inhibitor from the HeLa cell lysate after 5 h of incubation. Analysis by mass spectrometry showed the absence of dephosphorylation products or truncated versions of the molecule. In addition, the stability of **17** in HeLa cell lysate was analyzed using capillary electrophoresis (Figure 2). The peak intensities clearly showed that the intact inhibitor molecule is fully retained in the lysate.

Neither chain-truncation modification of **15**, the stereoinversion at the L-Thr($PO_3H_2$) residue nor the substitution of the $\beta$-(3-benzothienyl)alanine by phenylalanine could influence the domain selectivity of the inhibitor. This was confirmed by the 1:1 stoichiometry found with isothermal titration calorimetry (ITC) for complex formation of full-length *h*Pin1 with **17** and complex formation of **17** with the isolated PPIase domain, respectively. Furthermore, in both cases the ITC measurements revealed similar dissociation constants (19.3 $\pm$ 2.6 nM; 20.1 $\pm$ 2.3 nM). The $K_i$ value of **17** (Table 2), which was determined by concentration-dependent measurements of remaining Pin1 activity in the PPIase activity assay, was validated through ITC-measurements.

To test the specificity of the Pin1 inhibitors, other members of the PPIase class of enzymes (Par14, FKBP12, and Cyp18) as well as different protein kinases (ERK2, PKA, PKC) and protein phosphatases (PP2A, PP2B, PP1) were assayed in the presence of **16** and **17**, respectively. In the presence of 500 $\mu$M of either **16** or **17**, the observed inhibition of these enzymes did not exceed 10% in any case (see Supporting Information for experimental details).

To evaluate the effects of the inhibitor on the cell cycle, **17** and its nonphosphorylated derivative, respectively, were introduced into HeLa cells by electroporation using Amaxa technology (Amaxa, Cologne) and its effects on the cell cycle determined by flow cytometry analysis (see Supporting Information). Peptide **17** caused significant accumulation of cells in G2/M phase, but its nonphosphorylated derivative had no detectable effects. These results indicate that **17** specifically blocks HeLa cells in the G2/M phase, which is consistent with previous observations in experiments using antisense techniques.[6] To determine whether these growth inhibitory effects are dependent on the intracellular concentration of **17**, varying amounts of **17** were transfected into the cells using different concentrations of **17** during the electroporation procedure. The resulting intracellular concentrations of **17** were determined after cell lysis by HPLC. As shown in Figure 3, the cell cycle inhibitory effects of **17** were dose-dependent. The effective

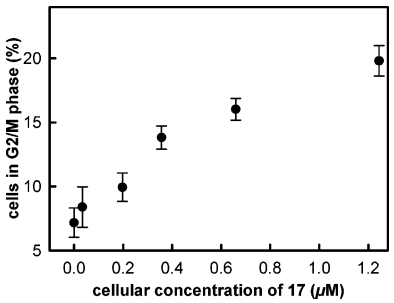


**Figure 3.** Specific inhibition of *h*Pin1 by **17** leads to an accumulation of HeLa cells in the G2/M phase. After transfection of different amounts of **17** into HeLa cells by electroporation, the cells were cultured for an additional 3 days at 37 °C. Cell cycle analysis was performed by determination of the intracellular DNA content using flow cytometry (experimental details are described in the Supporting Information). The fraction of cells in different cell cycle stages was calculated with ModFit LT 3.1 software. The cellular concentration of **17** was determined by cell lysis, centrifugation and subsequent analysis of the supernatant by reverse phase HPLC using a concentration standard graph of **17**. The cellular concentration of *h*Pin1 was determined to be 0.6 $\mu$M by Western blot analyses using HeLa cell lysates in combination with a concentration standard graph of the recombinant protein. In a control experiment the nonphosphorylated derivative of **17** was transfected into HeLa cells by electroporation, resulting in a cellular concentration of 1.4 $\mu$M. In that case, no influence on the cell cycle was observed (see Supporting Information).

concentration of **17** was in the range expected, considering the concentration of *h*Pin1 of about 0.6 $\mu$M in this cell type.[13] These results suggest that cellular *h*Pin1 can be inhibited to a sufficiently low level of activity by a highly potent, small-molecule inhibitor. The dose−response curve clearly showed a regulatory effect of the unblocked active site of Pin1 during cell cycle progression in HeLa cells.

In summary, we have successfully identified specific D-phosphothreonine-containing low-nanomolar inhibitors of *h*Pin1, using spot affinity evaluation of cellulose-bound peptide libraries. Far Western blot analyses and ITC measurements, respectively, revealed a complete discrimination in WW and PPIase domain binding. Clearly, the inhibitors compete with substrates for the catalytic site of the PPIase domain in a reversible manner and display significant stability in cell lysates. Moreover, the inhibitors block progression of HeLa cells through the G2/M phase in a dose-dependent manner. Therefore, the new inhibitors may prove useful in treating pathological conditions such as cancer where Pin1 is aberrantly upregulated.

**Acknowledgment.** We thank A. Schierhorn for mass spectroscopy and C. Lücke for NMR measurements. We are grateful for excellent technical assistance by B. Hökelmann, K. Jentzsch, K. Stein, and M. Heidler. The help of M. Weiwad in the kinase and phosphatase inhibition studies is gratefully acknowledged. We thank C. Schiene-Fischer and D. Ferrari for critical reading of the manuscript.

**Supporting Information Available:** Structures of the unnatural amino and *N*-alkyl amino acids, synthesis methods, Pin1-based screening of the cellulose-bound peptide libraries, and peptide analytics; enzyme assays and representative graphical cell cycle data; isothermal titration calorimetry. This material is available free of charge via Internet at http://pubs.acs.org.

## References

(1) Zhou, X. Z.; Kops, O.; Werner, A.; Lu, P. J.; Shen, M.; Stoller, G.; Küllertz, G.; Stark, M.; Fischer, G.; Lu, K. P. Pin1-dependent prolyl isomerization regulates dephosphorylation of Cdc25C and tau proteins. *Mol. Cell* **2000**, *6*, 873−883.

(2) Lu, K. P. Pinning down cell signaling, cancer and Alzheimer's disease. *Trends Biochem. Sci.* **2004**, *29*, 2000−209.

(3) Min, L.; Fulton, D. B.; Andreotti, A. H. A case study of proline isomerization in cell signalling. *Front. Biosci.* **2005**, *10*, 385−397.

(4) Yaffe, M. B.; Schutkowski, M.; Shen, M.; Zhou, X. Z.; Stukenberg, P. T.; Rahfeld, J. U.; Xu, J.; Kuang, J.; Kirschner, M. W.; Fischer, G.; Cantley, L. C.; Lu, K. P. Sequence-specific and phosphorylation-dependent proline isomerization: a potential mitotic regulatory mechanism. *Science* **1997**, *278*, 1957−1960.

(5) Schutkowski, M.; Bernhardt, A.; Zhou, X. Z.; Shen, M.; Reimer, U.; Rahfeld, J. U.; Lu, K. P.; Fischer, G. Role of phosphorylation in determining the backbone dynamics of the serine/threonine-proline motif and Pin1 substrate recognition. *Biochemistry* **1998**, *37*, 5566−5575.

(6) Lu, K. P.; Hanes, S. D.; Hunter, T. A human peptidyl-prolyl isomerase essential for regulation of mitosis. *Nature* **1996**, *380*, 544−547.

(7) Liou, Y. C.; Ryo, A.; Huang, H. K.; Lu, P. J.; Bronson, R.; Fujimori, F.; Uchida, T.; Hunter, T.; Lu, K. P. Loss of Pin1 function in the mouse causes phenotypes resembling cyclin D1-null phenotypes. *Proc. Natl. Acad. Sci. U.S.A.* **2002**, *99*, 1335−1340.

(8) Winkler, K. E.; Swenson, K. I.; Kornbluth, S.; Means, A. R. Requirement of the prolyl isomerase Pin1 for the replication checkpoint. *Science* **2000**, *287*, 1644−1647.

(9) Shen, Z. J.; Esnault, S.; Malter, J. S. The peptidyl-prolyl isomerase Pin1 regulates the stability of granulocyte-macrophage colony-stimulating factor mRNA in activated eosinophils. *Nat. Immunol.* **2005**, *6*, 1280−1287.

(10) Miyashita, H.; Mori, S.; Motegi, K.; Fukumoto, M.; Uchida, T. Pin1 is overexpressed in oral squamous cell carcinoma and its levels correlate with cyclin D1 overexpression. *Oncol. Rep.* **2003**, *10*, 455−461.

(11) Wulf, G.; Ryo, A.; Liou, Y.; Lu, K. P. The prolyl isomerase Pin1 in breast development and cancer. *Breast Cancer Res.* **2003**, *5*, 76−82.

(12) Ryo, A.; Uemura, H.; Ishiguro, H.; Saitoh, T.; Yamaguchi, A.; Perrem, K.; Kubota, Y.; Lu, K. P.; Aoki, I. Stable suppression of tumorigenicity by Pin1-targeted RNA interference in prostate cancer. *Clin. Cancer Res.* **2005**, *11*, 7523−7531.

(13) Rippmann, J. F.; Hobbie, S.; Daiber, C.; Guilliard, B.; Bauer, M.; Birk, J.; Nar, H.; Garin-Chesa, P.; Rettig, W. J.; Schnapp, A. Phosphorylation-dependent proline isomerization catalyzed by Pin1 is essential for tumor cell survival and entry into mitosis. *Cell Growth Differ.* **2000**, *11*, 409−416.

(14) Gemmill, T. R.; Wu, X. Y.; Hanes, S. D. Vanishingly low levels of Ess1 prolyl-isomerase activity are sufficient for growth in Saccharomyces cerevisiae. *J. Biol. Chem.* **2005**, *280*, 15510−15517.

(15) Zhang, Y.; Fussel, S.; Reimer, U.; Schutkowski, M.; Fischer, G. Substrate-based design of reversible Pin1 inhibitors. *Biochemistry* **2002**, *41*, 11868−11877.

(16) Wang, X. J.; Xu, B.; Mullins, A. B.; Neiler, F. K.; Etzkorn, F. A. Conformationally locked isostere of phosphoSer-cis-Pro inhibits Pin1 23-fold better than phosphoSer-trans-Pro isostere. *J. Am. Chem. Soc.* **2004**, *126*, 15533−15542.

(17) Uchida, T.; Takamiya, M.; Takahashi, M.; Miyashita, H.; Ikeda, H.; Terada, T.; Matsuo, Y.; Shirouzu, M.; Yokoyama, S.; Fujimori, F.; Hunter, T. Pin1 and Par14 Peptidyl Prolyl Isomerase Inhibitors Block Cell Proliferation. *Chem. Biol.* **2003**, *10*, 15−24.

(18) Hennig, L.; Christner, C.; Kipping, M.; Schelbert, B.; Rücknagel, K. P.; Grabley, S.; Küllertz, G.; Fischer, G. Selective inactivation of parvulin-like peptidyl-prolyl cis/trans isomerases by juglone. *Biochemistry* **1998**, *37*, 5953−5960.

(19) Chao, S. H.; Greenleaf, A. L.; Price, D. H. Juglone, an inhibitor of the peptidyl-prolyl isomerase Pin1, also directly blocks transcription. *Nucleic Acids Res.* **2001**, *29*, 767−773.

(20) Bayer, E.; Thutewohl, M.; Christner, C.; Tradler, T.; Osterkamp, F.; Waldmann, H.; Bayer, P. Identification of hPin1 inhibitors that induce apoptosis in a mammalian Ras transformed cell line. *Chem. Commun.* **2005**, *4*, 516−518.

(21) Smet, C.; Duckert, J. F.; Wieruszeski, J. M.; Landrieu, I.; Buee, L.; Lippens, G.; Deprez, B. Control of protein−protein interactions: Structure-based discovery of low molecular weight inhibitors of the interactions between Pin1 WW domain and phosphopeptides. *J. Med. Chem.* **2005**, *48*, 4815−4823.

JM060036N